energies

MDPI

Article

The Molecular Dynamics of Signature Gas Diffusions in Synthetic-Ester-Based Oil Under a Range of Thermal Conditions

Liping Guo [1], Hongliang Wang [1], Weiwei Qi [2], Jun Zhang [2] and Wu Lu [2,*]

[1] Shanghai Electric Transmission and Distribution Experimental Center Co., Ltd., Shanghai 200072, China
[2] College of Electrical Engineering, Shanghai University of Electric Power, Shanghai 200090, China
* Correspondence: wuluee@shiep.edu.cn

Abstract

Synthetic ester insulating oils are extensively utilized in power transformers due to their exceptional insulating properties, thermal stability, and environmental compatibility. The dissolved gas analysis (DGA) technique, which is employed to diagnose internal faults in transformers by monitoring the concentration and composition of dissolved gases in oil, is thought to be effective in detecting typical faults such as overheating and partial discharges in synthetic esters. However, owing to the significant differences in the properties of traditional mineral oil and synthetic esters, the existing DGA-based diagnostic methods developed for mineral oils cannot be directly applied to synthetic esters. A deep understanding of the microscopic processes occurring during the gas generation and diffusion of synthetic esters is an urgent necessity for DGA applications. Therefore, in this study, we systematically investigated the diffusion behavior of seven typical fault gases in synthetic ester insulating oils within a temperature range of 343–473 K using molecular dynamics simulations. The results demonstrate that H_2 exhibits the highest diffusion capability across all temperatures, with a diffusion coefficient of 33.430 $\times$ 10^{-6} cm^2/s at 343 K, increasing to 402.763 $\times$ 10^{-6} cm^2/s at 473 K. Additionally, this paper explores the microscopic mechanisms underlying the diffusion characteristics of these characteristic gases by integrating the Free-Volume Theory, thereby providing a theoretical foundation for refining the fault gas analysis methodology for transformer insulating oils.

Keywords: synthetic ester; dissolved gas analysis; molecular dynamics; diffusion coefficient; free volume

check for updates

Academic Editor: Bohung Kim

Received: 27 April 2025
Revised: 3 June 2025
Accepted: 4 June 2025
Published: 23 June 2025

Citation: Guo, L.; Wang, H.; Qi, W.; Zhang, J.; Lu, W. The Molecular Dynamics of Signature Gas Diffusions in Synthetic-Ester-Based Oil Under a Range of Thermal Conditions. *Energies* **2025**, *18*, 3276. https://doi.org/10.3390/en18133276

Copyright: © 2025 by the authors. Licensee MDPI, Basel, Switzerland. This article is an open access article distributed under the terms and conditions of the Creative Commons Attribution (CC BY) license (https://creativecommons.org/licenses/by/4.0/).

1. Introduction

As the global energy system is showing a low-carbon and environmentally sustainable trend, the demand for sustainable and high-performance insulating materials for power equipment is becoming increasingly critical. Synthetic ester insulating oils, characterized by their high ignition points, biodegradability, excellent dielectric strength, and thermal stability, have emerged as promising alternatives to traditional mineral oils, particularly for power transformers with stringent environmental requirements as well as high-voltage and large-capacity applications, offering significant advantages [1,2]. Despite the excellent performance of synthetic esters in terms of environmental friendliness and thermal stability, the characteristic gas diffusion mechanism of synthetic ester oils under the influence of typical internal discharge or overheating faults in transformers is still unclear, which has led to the challenge of fault diagnosis based on the dissolved gas analysis (DGA) technique in oil. Furthermore, the diagnostic criteria of traditional DGA methods are based on

mineral oil systems, whereas the diffusion behavior and equilibrium characteristics of dissolved gases in synthetic esters may differ markedly from those in mineral oils due to inherent differences in viscosity, polarity, and molecular structure. Direct application of the existing diagnostic criteria may lead to underestimation or misjudgment of gas concentration thresholds and increase the risk of fault misdiagnosis due to discrepancies in diffusion kinetics. Therefore, there is an urgent need to elucidate the diffusion mechanisms of characteristic gases in synthetic esters, as doing so would contribute to the refinement and optimization of fault diagnosis methods for synthetic-ester-immersed transformers based on DGA technology [3–6].

Recent research on synthetic esters has predominantly focused on optimizing their electrical properties, thermal aging characteristics, and compatibility with solid insulating materials. Studies have demonstrated that synthetic esters exhibit superior dielectric strength and lower dielectric loss compared to mineral oils, along with a slower increase in acid value during prolonged thermal aging [7,8]. Additionally, synthetic esters show enhanced compatibility with cellulose insulating paper, which helps mitigate the aging of an insulating material [9,10], and their oxidative stability at elevated temperatures is significantly superior to that of mineral oils [11]. However, most of the existing studies have concentrated on macroscopic physical parameters (e.g., dielectric constant, viscosity, etc.) and analyses of aging products, with limited attention given to the systematic exploration of the diffusion kinetics of dissolved gases within the synthetic ester system [12,13]. Although a few experimental investigations have compared the gas solubility differences between synthetic esters and mineral oils, the experimental conditions often hinder the elucidation of the diffusion mechanism at the molecular level, resulting in an incomplete understanding of migration patterns [14].

In the DGA technique, internal transformer faults are diagnosed by monitoring the concentration and proportion of dissolved gases in the oil, and the technique's effectiveness relies on an accurate knowledge of the gas diffusion mechanism [15]. At present, the traditional DGA technique based on mineral oil is highly mature, and its diagnostic logic and gas concentration thresholds have been fully verified through long-term engineering practice, but such methods are not directly applicable to the fault analysis of natural ester insulating oils, and it is doubtful whether this technique's theoretical framework is applicable to synthetic ester systems [16,17]. In view of the characteristics of natural ester insulating oils, some scholars preliminarily explored the DGA diagnostic framework adapted to natural esters by experimentally modifying the gas solubility parameter and adjusting the threshold value of the proportion of fault gases [18–20]. However, despite some scholars' attempts to experimentally study the macroscopic characteristics of synthetic esters, there is a lack of studies determining their characteristic gas diffusion behaviors and gas diffusion kinetic mechanisms. These bottlenecks have constrained the development of DGA diagnostic criteria applicable to synthetic esters, and there is an urgent need to reveal the gas diffusion mechanisms of synthetic esters at the molecular dynamics level [21–23].

To address the above issues, we employed molecular dynamics simulations to systematically investigate the diffusion behaviors of seven typical fault-characteristic gases in synthetic ester insulating oil within the temperature range of 343 K to 473 K. Utilizing the molecular dynamics simulation approach, a synthetic ester molecular model and a gas miscible system were developed. This study further examines the influence mechanism of temperature gradients on the gas diffusion behavior of the insulating oil at the microscopic level through the calculation of mean square displacements (MSDs) and gas diffusion coefficients in conjunction with the free-volume theory. The findings of this research can be applied to the design optimization of DGA technology for synthetic ester insulating oils,

thereby facilitating the reliable operation and intelligent maintenance of environmentally friendly transformers.

2. Simulation Methodology

2.1. Molecular Diffusion Modeling of Synthetic Esters

We constructed a molecular dynamics model of a synthetic ester composed of Pentaerythritol tetranonanoate (PENTA-TNA, $C_{41}H_{76}O_8$) and its composite system with fault-characteristic gases. The structure of a single synthetic ester molecule consists of a pentaerythritol backbone and four isononyl ester groups, which confer excellent thermal stability and outstanding electrical properties. To accurately characterize the macroscopic properties of this system, an initial model was constructed using 10 PENTA-TNA molecules, and periodic boundary conditions were applied to eliminate size effects. Furthermore, multi-stage dynamic relaxation and geometric optimization were performed to eliminate potential atomic-level anomalous contact and high-energy configurations in the initial model, facilitating the model's stabilization to a reasonable state. Specifically, the steps include achieving a 100 ps thermal equilibrium under the NPT ensemble, realizing 100 ps energy stabilization under the NVE ensemble, pressure adjustment under the low-pressure NPT ensemble, and 10,000-step geometric optimization based on the conjugate gradient method. After carrying out these optimization steps, the final PENTA-TNA molecular model, with a unit cell length of 23.28 Å and a density of 0.917 g/cm^3, was obtained, as shown in Figure 1.

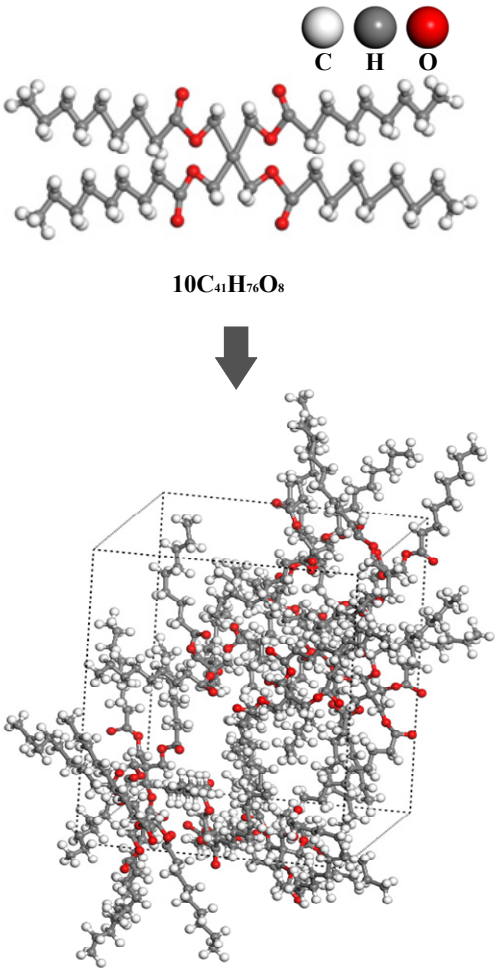


Figure 1. Molecular modeling of a synthetic ester.

In this study on the diffusion behavior of dissolved gases in oil, a composite molecular model containing seven characteristic gases was constructed based on the PENTA-TNA base oil model. During the construction of the molecular models for small gas molecules using Materials Studio, small gas molecules and synthetic ester molecules were differentiated by color: C in the small gas molecules was colored dark gray, H was given in emerald green, and O was given in light blue. As shown in Figure 2, these molecular models are complete and strictly adhere to the standard requirements for initial configurations in molecular dynamics simulations. In this study, 10 gas molecules were randomly embedded in the base oil model formed by 10 PENTA-TNA molecules, and the overall density was set to 0.95 g/cm^3 to match the physical property requirements under actual operating conditions. As exemplified by the CH_4 diffusion model shown in Figure 3, this system maintains the stable configuration of the base oil while ensuring accurate description of short-range interactions, such as van der Waals forces, through reasonable molecular spacing.

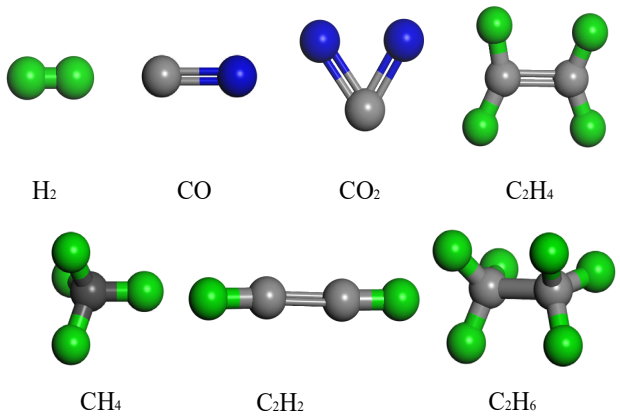


Figure 2. Gas molecule modeling.

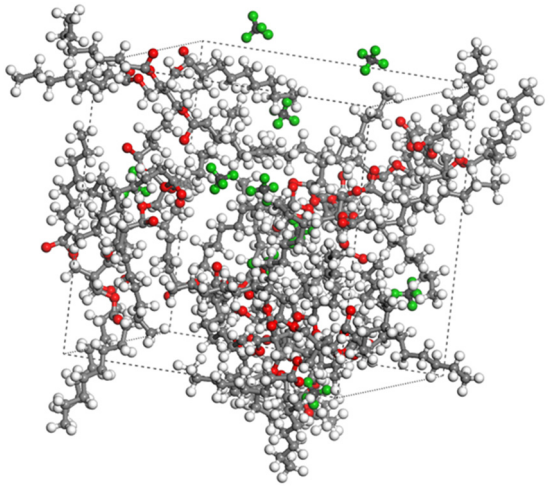


Figure 3. Molecular modeling of mixed oil-and-gas system. (Hydrogen and carbon atoms in CH_4 are shown in green and gray, respectively, and oxygen, hydrogen, and carbon atoms in the molecule are shown in red, gray, and white, respectively).

2.2. Simulation Parameter Settings

We constructed a computational framework based on the PCFF force field to simulate the diffusion behavior of dissolved gases in synthetic esters using molecular dynamics. The force field builds upon the core parameters of the CFF91 force field and significantly enhances simulation accuracy for complex organic molecular systems by extending the functional expressions for bond length vibration, bond angle bending, dihedral torsion, and

non-bond interactions in polymeric systems. To address the non-bond interactions between the synthetic ester and gas molecules, the van der Waals forces were computed using the Atom-Based truncation method, which reduces computational load within a reasonable range and improves simulation efficiency. The electrostatic interactions are handled using the Ewald summation method, which accurately describes long-range Coulomb forces while also maintaining computational efficiency.

Additionally, in terms of thermodynamic control algorithms, a hierarchical multi-level control approach was applied. Firstly, temperature regulation was achieved through the Andersen thermostat algorithm, whose random collision mechanism effectively maintained the thermal equilibrium of the system and prevented local thermal anomalies. Secondly, pressure control was carried out using the Berendsen method, ensuring stable convergence of the system under a standard pressure of 0.1 MPa, thereby simulating the actual working environment of transformers. Lastly, the Velocity Verlet algorithm was employed for dynamic integration, balancing energy conservation with trajectory accuracy to ensure the authenticity of molecular motion behavior. The three-dimensional system constructed during the simulations mitigates finite-size effects by employing periodic boundary conditions, which enables a more accurate simulation of molecular diffusion behavior in real oils [24,25].

Before conducting molecular dynamics simulations, it is essential to optimize the geometric structure of a system and relax the pressure. Specifically, the process is divided into the following steps:

(1) A preliminary composite model of synthetic ester oil molecules and gas molecules is constructed and undergoes 10,000 steps of geometric structure optimization to eliminate potential atomic overlaps and non-physical contact.
(2) Pressure relaxation is performed under the NPT ensemble for 100 ps to allow the system's density to converge to 0.95 g/cm^3, ensuring the accuracy of subsequent simulations.

After the above steps were completed, a 600 ps molecular dynamics simulation was carried out under the NVT ensemble conditions. The simulation process was divided into two parts: the first 100 ps were used to achieve a stable molecular state, and the remaining 500 ps were used for data collection to analyze the diffusion characteristics of dissolved gas molecules. The recording interval of the molecular trajectory was reduced to 1 ps in order to capture the complete gas diffusion process, providing a reliable data foundation for the calculation of diffusion coefficients.

Furthermore, considering that the actual operating temperature of transformer insulating oil typically ranges from 313 K to 423 K, four simulation temperatures were selected to represent different operating conditions pertaining to the transformer: 343 K represents the normal operating state; 393 K represents the temperature under high load or mild overheating conditions; 423 K corresponds to the early stage of thermal failure; and 473 K represents a high temperature close to the point of discharge failure. By performing molecular dynamics simulations under these temperature conditions, the diffusion coefficients of each characteristic gas in synthetic ester were calculated, and the micro-mechanisms of the effect of temperature on the diffusion characteristics of the gases were analyzed in combination with the free volume, which provides data support for the optimization of DGA technology.

3. Results and Discussion

3.1. Characteristic Gas Diffusion Properties

In the synthetic ester system, the diffusion characteristics of gas molecules of different types exhibit significant differences. This study utilizes the mean squared displacement (MSD) curve to clearly describe the diffusion characteristics of gases in the oil and their

correlations with temperature. According to molecular dynamics theory, the mean squared displacement is defined as the statistical average of the deviation of the positions of all particles in the system relative to a reference position over a time interval t. The expression is given below:

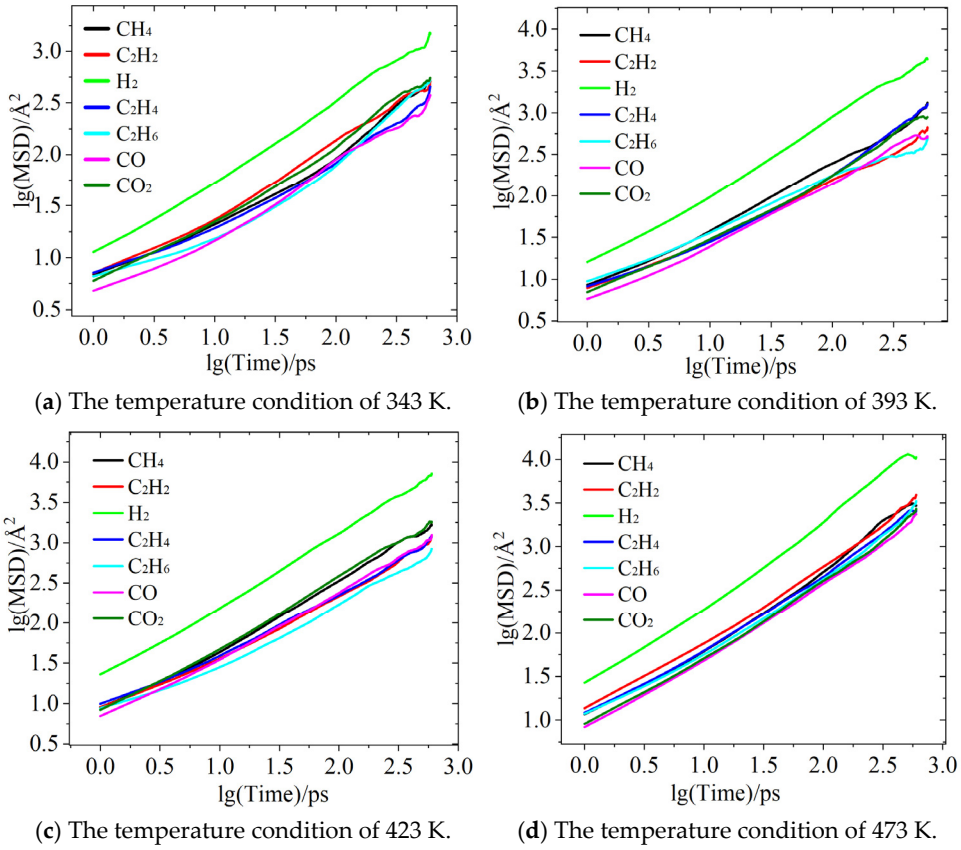
$$MSD(t) = \left\langle \left| r(t) - r(0) \right|^2 \right\rangle \quad (1)$$

where $r(t)$ is the particle's position at a given time, $r(0)$ is the initial reference position, and $\langle X \rangle$ represents the statistical average within the system.

Figure 4 presents a schematic of the mean squared displacement (MSD) for various characteristic gases, depicted using a log–log dependence. Of all the gasses, H_2 demonstrates the strongest diffusion ability under all temperature conditions, maintaining the highest mean squared displacement (MSD) compared to the other gases. This is primarily attributed to the minimal molecular weight of H_2, provoking the least resistance from oil molecules, as well as the pronounced effect of temperature increases on enhancing its diffusion capacity. As depicted in Figure 4a,b, at 343 K, the MSD of H_2 is an order of magnitude higher than that of the other gases, and as the temperature rises to 473 K, its diffusion advantage remains evident. This reflects the highly efficient diffusion characteristics of lightweight non-polar molecules in synthetic esters. Additionally, in the later stages of hydrogen diffusion, deviations from the mean squared displacement (MSD) curve can be observed under varying temperature conditions. For instance, as shown in Figure 4a, the tail of the curve exhibits a sharp upward trend, whereas in Figure 4d, the tail demonstrates a sudden decline. This phenomenon can be attributed to two factors: first, the exceptionally high diffusion ability of H_2 molecules, which makes them more susceptible to thermal fluctuations or boundary effects in small-scale systems, and, second, the limited number of particles within the simulated system, making the system prone to inducing statistical fluctuations, particularly for highly diffusive gases.

For the gases CO and CO_2 oxide, the MSD of CO_2 is consistently higher than that of CO, with the difference being particularly noticeable at lower temperatures. However, as the temperature increases, the diffusion capabilities of the two gases gradually converge. For example, at 473 K, the MSD of CO_2 is only slightly higher than that of CO. This phenomenon could be attributed to the increased thermal motion of oil molecules at higher temperatures, which reduces the system's viscosity and thus diminishes the impact of molecular weight differences on diffusion. Furthermore, the diffusion processes of CO and CO_2 are primarily dominated by the physical properties of the insulating oil, as their polar nature leads to lower solubility in weakly polar synthetic ester oils.

In addition, the diffusion characteristics of hydrocarbon gases exhibit complex temperature sensitivity. At 343 K, C_2H_2 has the highest MSD, indicating that, under this temperature condition, its diffusion ability is the strongest among hydrocarbon gases. This may be related to the lower spatial hindrance resulting from its linear molecular structure, as shown in Figure 4a. As shown in Figure 4b, when the temperature rises to 393 K, C_2H_4 exhibits the highest MSD among hydrocarbon gases, likely due to its double-bond structure, which allows intermolecular forces to be overcome at higher temperatures. Figure 4c,d reveal that CH_4 shows a significant enhancement in diffusion ability at higher temperatures (423–473 K), possibly due to the decrease in synthetic ester viscosity during the temperature rise, with the simple spherical molecular structure of CH_4 benefiting the most from this decrease. However, C_2H_6 consistently demonstrated the slowest diffusion rate among the hydrocarbon gases, likely due to the inhibitory effect of its greater molecular weight and branched structure. This variation in diffusion order under different temperature conditions suggests that the diffusion characteristics of hydrocarbon gases are not only closely related to temperature but also influenced by the molecular structure of each gas, intermolecular interactions, and solubility in the oil.



(**a**) The temperature condition of 343 K. (**b**) The temperature condition of 393 K.

(**c**) The temperature condition of 423 K. (**d**) The temperature condition of 473 K.

Figure 4. MSD plots of diffusion behavior of characteristic gases.

Overall, the diffusion abilities of characteristic gases align with the following trend: H_2 > hydrocarbon gases > CO and CO_2. However, the relative diffusion capabilities fluctuate dynamically with temperature. Moreover, the diffusion characteristics are determined by factors such as molecular weight, polarity, molecular structure, and the properties of insulating oils. The exceptional diffusion ability of H_2 is primarily attributed to its extremely low molecular weight, while the complex temperature-dependent behavior of hydrocarbon gases reveals the influence of molecular structure on the diffusion process. The findings of this study provide an important theoretical basis for optimizing gas-monitoring technologies based on diffusion characteristics.

3.2. Characteristic Gas Diffusion Coefficient

The diffusion coefficient is a key parameter for quantitatively describing the migration ability of gas molecules in insulating oils, and it is calculated based on the linear relationship between the mean squared displacement (MSD) and time. By analyzing the MSD curves in Figure 4, it can be observed that within the time range of 25 ps to 500 ps, the MSD of all the gases exhibits a strong linear relationship with time, indicating that molecular motion is primarily governed by free diffusion during this period. To accurately calculate the diffusion coefficient (D), it is necessary to select the linear segment of the MSD curve for linear regression fitting. The slope (k) obtained from this fitting is then used to establish a quantitative relationship with the diffusion coefficient:

$$D = \frac{k}{6} \tag{2}$$

where the coefficient 6 indicates that the diffusion system is three-dimensional.

Additionally, the goodness of fit for the linear regression is represented by the correlation coefficient R^2, and it can be calculated using the following formula:

$$R^2 = 1 - \frac{\sum (l_i - \hat{l}_i)^2}{\sum (l_i - \bar{l})^2} \quad (3)$$

where l_i represents the actual MSD values; $\hat{l}_i$ represents the fitted MSD values; and $\bar{l}$ represents the mean MSD values.

Based on the aforementioned method and by combining the MSD values of the characteristic gases, the diffusion coefficients of seven characteristic gases in the synthetic ester were calculated at four different temperatures: 343 K, 393 K, 423 K, and 473 K. The results reveal the temperature-dependent behavior of gas diffusion and its correlation with molecular characteristics. As shown in Table 1, the diffusion coefficients of the characteristic gases significantly increased when increasing the temperature, with H_2 exhibiting the most notable diffusion capacity. At 343 K, the diffusion coefficient of H_2 was 33.430 $\times$ 10^{-6} cm^2/s, and as the temperature increased, it rose to 402.763 $\times$ 10^{-6} cm^2/s at 473 K, marking a 12-fold increase, far exceeding that of the other gases. This can be attributed to the extremely low molecular weight of H_2 and its weak intermolecular forces, making it highly sensitive to temperature changes.

Table 1. Characteristic gas diffusion coefficients at four temperatures.

		H_2	CO	C_2H_2	CH_4	CO_2	C_2H_6	C_2H_4
343 K	Slope, k	2.006	0.434	0.799	0.862	0.943	0.918	0.539
	Fitted correlation coefficient, R^2	0.976	0.980	0.987	0.991	0.973	0.998	0.990
	Diffusion coefficient D/$\times 10^{-6}$ cm^2/s	33.430	7.225	8.992	14.365	15.722	15.295	8.992
393 K	Slope, k	6.936	1.087	2.010	1.627	1.786	0.511	2.010
	Fitted correlation coefficient, R^2	0.990	0.994	0.994	0.990	0.997	0.926	0.999
	Diffusion coefficient D/$\times 10^{-6}$ cm^2/s	115.607	18.113	13.915	27.112	29.770	8.510	33.494
423 K	Slope, k	10.911	1.804	1.809	2.665	2.656	1.114	1.685
	Fitted correlation coefficient, R^2	0.994	0.994	0.993	0.972	0.981	0.988	0.992
	Diffusion coefficient D/$\times 10^{-6}$ cm^2/s	181.85	30.074	30.154	44.410	44.263	18.559	28.088
473 K	Slope, k	24.166	3.377	5.983	6.187	3.998	4.411	4.741
	Fitted correlation coefficient, R^2	0.999	0.998	0.992	0.995	0.990	0.997	0.997
	Diffusion coefficient D/$\times 10^{-6}$ cm^2/s	402.763	56.278	99.719	103.119	66.631	73.524	79.014

Hydrocarbon gases such as CH_4, C_2H_2, C_2H_4, and C_2H_6 also exhibited significant increases in diffusion coefficients at 473 K compared to the values at 343 K, surpassing 70 $\times$ 10^{-6} cm^2/s. For example, the diffusion coefficient of CH_4 increased from 14.365 $\times$ 10^{-6} cm^2/s to 103.119 $\times$ 10^{-6} cm^2/s. Among these gases, C_2H_2 showed the most significant temperature-dependent diffusion change, with its diffusion coefficient increasing from 18.992 $\times$ 10^{-6} cm^2/s to 99.719 $\times$ 10^{-6} cm^2/s, indicating that its linear molecular structure allows for more efficient diffusion into the insulating oil at higher temperatures. In contrast, oxide gases such as CO and CO_2 exhibited lower diffusion coefficients than H_2 and hydrocarbons but still showed a steady increasing trend. The diffusion coefficient of CO_2 increased from 15.722 $\times$ 10^{-6} cm^2/s at 343 K to 66.631 $\times$ 10^{-6} cm^2/s at 473 K, while that of CO increased from 7.225 $\times$ 10^{-6} cm^2/s to 56.278 $\times$ 10^{-6} cm^2/s, with growth factors of 4.2 and 7.8, respectively.

Furthermore, the behavior of the diffusion process can be further characterized by the slope, k. The data shows that the diffusion behavior of the characteristic gases intensifies with an increase in temperature. It is noteworthy that the slope for C_2H_6 exhibited an unusual decrease at 393 K (0.511) but recovered and resumed growth at higher temperatures, suggesting that the molecular interactions or solubility of C_2H_6 might change in this specific

temperature range, temporarily inhibiting its diffusion. The reliability of the diffusion model was verified through the fitting correlation coefficient (R^2), particularly at 473 K, where all the gases exhibited R^2 values above 0.99, confirming that the constructed diffusion model effectively describes the diffusion characteristics of the characteristic gases.

In conclusion, the relative strength of gas diffusion and its temperature response characteristics provide a reference for the dynamic monitoring of dissolved gases in transformer insulating oil. For example, the highly sensitive diffusion characteristics of H_2 at high temperatures highlight its potential advantage in early fault warning. These findings foster a deeper understanding of the diffusion mechanisms of gases in insulating oil from a molecular dynamics' theory, laying a theoretical foundation for optimizing DGA-based detection technologies based on diffusion characteristics.

3.3. Analysis of the Free Volume

The Free-Volume Theory (FVT) is an important theoretical model used to explain the diffusion behavior of molecules in liquids or polymers. Its core assumption is that there are unoccupied spaces within a liquid, referred to as free volume (V_F). The free volume arises from the random motion of molecules and provides the spatial channels required for the migration of gas molecules. In addition, the free volume of a gas molecule is affected by the nature and size of the molecule. The free-volume fraction (FFV) is obtained by calculating the ratio of free volume to total volume. Also, the free-volume fraction (FFV) is temperature-dependent; as the degree of thermal motion of molecules increases, the free-volume fraction within the system also increases, thereby enhancing the diffusion capacity of gases [26,27]. The expression for the free-volume fraction is

$$FFV = \frac{V_F}{(V_O + V_F)} \tag{4}$$

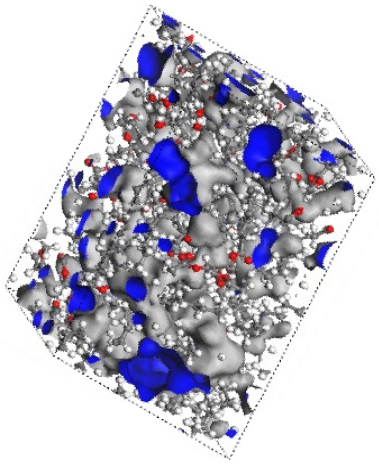
where V_O is the total volume of the system.

Based on the Free-Volume Theory (FVT), we quantitatively analyzed the free-volume characteristics of the synthetic ester and characteristic gas mixture system in the temperature range of 343 K to 473 K using the Connolly surface method and the Atom Volume and Surface tool in Materials Studio software 2020.

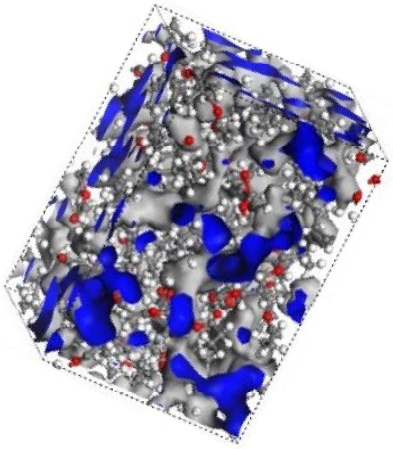
As shown in Table 2, as the temperature increases from 343 K to 473 K, the V_O value slightly decreases, while the V_F value significantly increases, leading to an increase in FFV from 0.20–0.25 to 0.31–0.37. This indicates that with the rise in temperature, the thermal motion of the oil molecules intensifies, enlarging the intermolecular gaps and forming more interconnected free-volume regions. As illustrated in Figure 5a–d, the blue regions in the figures represent the free-volume regions, which provide more favorable pathways for gas diffusion. As shown in Figure 5a,d, at 343 K, the distribution of free volume is sparse, and the FFV of H_2 is only 0.20. However, at 473 K, the free-volume region reaches a maximum, and the connectivity of the blue areas is enhanced. As shown in Figure 6a, the FFV of H_2 increases to 0.31, corresponding to an almost 11-fold increase in its diffusion coefficient. This suggests that at higher temperatures, the molecular model of the synthetic ester shows a significant increase in the intermolecular gaps, facilitating the diffusion of H_2 in the insulating oil.

Table 2. Free volume fraction coefficients at four temperatures.

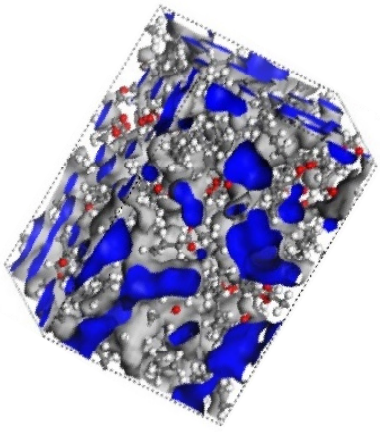
		H_2	CO	C_2H_2	CH_4	CO_2	C_2H_6	C_2H_4
343 K	$V_O/Å^3$	10,350.02	10,485.33	10,533.40	10,529.35	10,505.37	10,666.58	10,625.38
	$V_F/Å^3$	2646.90	3142.39	3464.01	3269.71	3281.19	3356.80	3195.41
	FFV	0.20	0.23	0.25	0.24	0.24	0.24	0.23
393 K	$V_O/Å^3$	10,160.35	10,393.38	10,427.70	10,257.76	10,396.42	10,531.99	10,533.93
	$V_F/Å^3$	3372.90	3366.26	3770.76	4197.00	3944.10	4437.33	3675.62
	FFV	0.25	0.24	0.27	0.29	0.28	0.30	0.26
423 K	$V_O/Å^3$	10,104.14	10,371.54	10,459.69	10,437.51	10,300.77	10,447.81	10,475.45
	$V_F/Å^3$	4037.57	3794.67	3797.13	3965.30	4510.79	4450.45	4269.83
	FFV	0.29	0.27	0.27	0.28	0.30	0.30	0.29
473 K	$V_O/Å^3$	10,004.15	10,161.04	10,069.42	10,126.33	10,319.65	10,322.82	10,165.65
	$V_F/Å^3$	4418.79	4601.97	5883.93	4889.77	4559.66	5706.45	5360.52
	FFV	0.31	0.31	0.37	0.33	0.31	0.36	0.35



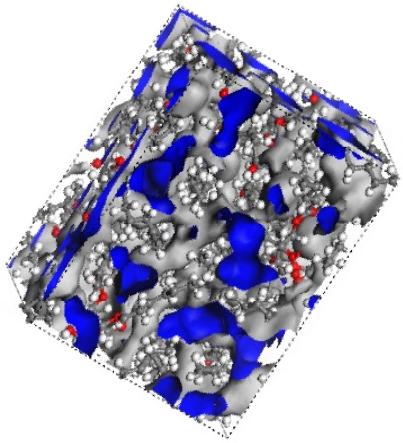
(**a**) The temperature condition of 343 K.



(**b**) The temperature condition of 393 K.

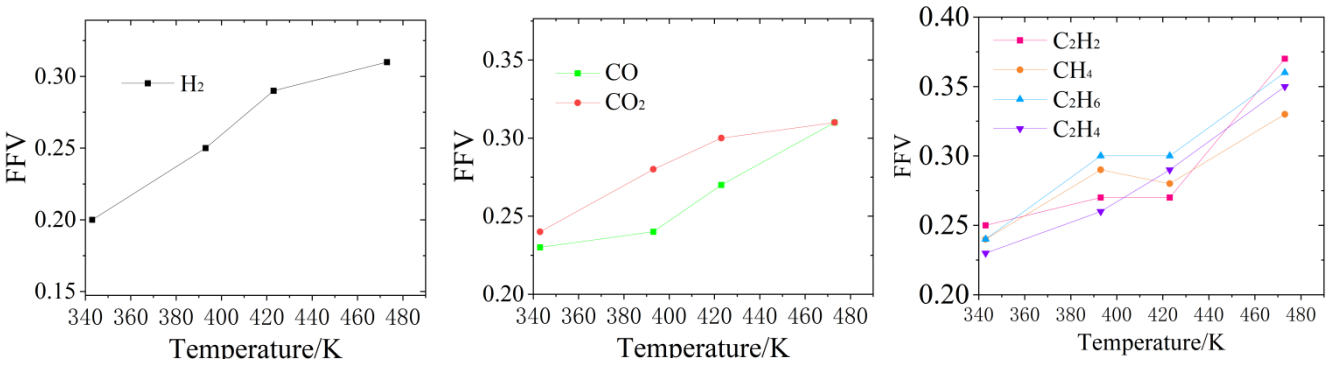


(**c**) The temperature condition of 423 K.



(**d**) The temperature condition of 473 K.

Figure 5. Free-volume modeling of H_2 gas in synthetic ester oils under different temperature conditions. (The blue color in the figure indicates the free volume region in the molecular model).



(**a**) FFV for monomolecular gas (**b**) FFV for oxide gases (**c**) FFV for hydrocarbon gases

Figure 6. Trends in FFV values in molecular modeling.

Further analysis of the free-volume variation characteristics of different gases reveals that these characteristics are closely related to the molecular properties of each gas. For small-molecule gases such as H_2 and CO, the FFV is relatively low at low temperatures, being 0.20 and 0.23, respectively, at 343 K. However, at high temperatures, the increase is significant, reaching 0.31 at 473 K, which is consistent with the trend of their diffusion coefficients. In the case of hydrocarbon gases, C_2H_2 exhibits a significantly higher FFV of 0.37 at 473 K due to its high polarity and weak intermolecular interactions, as shown in Figure 6c, so it more easily diffuses into the free-volume regions at higher temperatures in comparison to other hydrocarbons. Although CO_2 also exhibits an increase in FFV to 0.31 at high temperatures, its diffusion coefficient increase is relatively low due to its larger molecular size and stronger intermolecular forces, as shown in Figure 6b.

From the above analysis, it can be concluded that the increase in FFV directly reduces the diffusion resistance of gas molecules. For example, the 12-fold increase in the diffusion coefficient of H_2 corresponds to a 55% increase in its FFV. Furthermore, the variation in the FFV for different gases is in general agreement with the variation in their diffusion coefficients. Therefore, the strong correlation between the free-volume model and the diffusion data validates the applicability of the Free-Volume Theory (FVT) to explaining gas diffusion behavior in synthetic esters. This analysis not only clarifies the microscopic mechanism of temperature's influence on gas diffusion ability but also provides a theoretical basis for revising fault gas analysis methods in transformer insulating oils.

4. Conclusions

In this study, based on molecular models of synthetic esters and characteristic gas molecules constructed using the Materials Studio platform, we employed the PCFF force field and thermodynamic algorithms to quantitatively characterize the diffusion coefficients and free-volume distribution characteristics of gases at various temperatures. Additionally, by integrating molecular dynamics simulations with Free-Volume Theory, the diffusion mechanisms and temperature-dependent behaviors of seven characteristic gases (H_2, CH_4, C_2H_2, C_2H_4, C_2H_6, CO, and CO_2) in synthetic esters were systematically examined within the temperature range of 343–473 K. The results reveal the following.

(1) Under varying temperature conditions, the diffusion coefficients of all the gases studied exhibit a nonlinear increase with an increase in temperature. Hydrogen gas (H_2), due to its extremely low molecular weight and weak intermolecular forces, shows a dramatic increase in the diffusion coefficient, from 33.430×10^{-6} cm^2/s at 343 K to 402.763×10^{-6} cm^2/s at 473 K, reflecting a 12-fold increase. This rate of increase is significantly higher than that observed for the other gases. Among the hydrocarbons, C_2H_2, with its linear molecular structure, demonstrates a notable

advantage in diffusion at elevated temperatures, reaching 99.719 × 10^{-6} cm^2/s at 473 K.

(2) As the temperature increases, the free-volume fraction (FFV) of each molecular system rises substantially, ranging from 0.20 to 0.37. This increase is primarily due to thermal effects, which expand the intermolecular gaps and diffusion channels, thereby reducing resistance to gas migration. Furthermore, by correlating changes in diffusion coefficients with variations in FFV, it was observed that the 12-fold increase in the diffusion coefficient of H_2 corresponds to a 55% increase in its FFV. This correlation further substantiates the applicability of Free-Volume Theory (FVT) in explaining the diffusion behavior of gases in synthetic esters.

This paper fosters a deeper understanding of the gas diffusion mechanisms in synthetic esters at the molecular scale, offering theoretical insights for the enhancement of fault gas analysis methods in transformer insulating oils. It contributes to improving the efficiency of monitoring the operational status of power equipment, thereby enhancing the safety and stability of power systems.

Author Contributions: Conceptualization, L.G. and H.W.; methodology, W.Q. and W.L.; software, W.Q.; validation, W.L. and J.Z.; formal analysis, J.Z.; investigation, W.Q. and J.Z.; resources, H.W.; data curation, L.G.; writing—original draft preparation, J.Z.; writing—review and editing, L.G.; supervision, H.W. All authors have read and agreed to the published version of the manuscript.

Funding: This paper received no additional funding or sponsorship.

Data Availability Statement: The data that support the findings of this study are available from the corresponding author upon reasonable request.

Conflicts of Interest: Authors Liping Guo and Hongliang Wang were employed by the company Shanghai Electric Transmission and Distribution Experimental Center Co., Ltd. The remaining authors declare that the research was conducted in the absence of any commercial or financial relationships that could be construed as a potential conflict of interest.

References

1. Jovalekic, M.; Vukovic, D.; Tenbohlen, S. Gassing behavior of various alternative insulating liquids under thermal and electrical stress. In Proceedings of the IEEE International Symposium on Electrical Insulation, San Juan, Puerto Rico, 10–13 June 2012.
2. Li, D.; Rao, X.; Zhang, L.; Zhang, Y.; Ma, S.; Chen, L.; Yu, Z. First-Principle Insight into the Ru-Doped PtSe2 Monolayer for Detection of H2 and C2H2 in Transformer Oil. *ACS Omega* **2020**, *5*, 31872–31879. [CrossRef] [PubMed]
3. Liao, Y.; Zhou, Q.; Hou, W.; Li, J.; Zeng, W. Theoretical study of dissolved gas molecules in transformer oil adsorbed on intrinsic and Cr-doped InP3 monolayer. *Appl. Surf. Sci.* **2021**, *561*, 149816. [CrossRef]
4. Wang, J.; Zhang, X.; Liu, L.; Wang, Z. Dissolved gas analysis in transformer oil using Ni-Doped GaN monolayer: A DFT study. *Superlattices Microstruct.* **2021**, *159*, 107055. [CrossRef]
5. Fan, X.; Luo, H.; Liang, F.; Hu, J.; Liu, W.; Li, C.; He, J. Photon Count Technique as a Potential Tool for Insulation Micro-Defect Detection: Principles and Primary Results. *iEnergy* **2023**, *2*, 258–263. [CrossRef]
6. Fan, X.; Niu, S.; Luo, H.; Liang, J.; Liu, F.; Li, W.; Liu, W.; Gao, W.; Huang, Y.; Li, C.; et al. Photon counting technique as a potential tool in micro-defect detection of epoxy insulation pull rod in gas-insulated switchgears. *High Volt.* **2024**, *9*, 267–274. [CrossRef]
7. Jayyid, U.L.; Fadillah, A.; Kurniawan, M.; Suwarno; Rachmawati; Lesmana, A.; Mutia, S.; Anwar, A. Comparative Study of Mineral Oil, Synthetic Ester, and Natural Ester as Liquid Insulation in Transformers. In Proceedings of the 2024 6th International Conference on Power Engineering and Renewable Energy (ICPERE), Bandung, Indonesia, 5–6 November 2024.
8. Lee, S.; Jeong, H.; Park, J.; Seok, B.Y.; Ryu, J.; Bae, C. Research on Dielectric Strength Properties of Synthetic Ester Oil. In Proceedings of the 2024 10th International Conference on Condition Monitoring and Diagnosis (CMD), Gangneung, Republic of Korea, 20–24 October 2024.
9. Guerbas, F.; Adjaout, L.; Abada, A.; Rahal, D. New and Reclamation Transformer Oil Behavior under Accelerated Thermal Aging. In Proceedings of the IEEE International Conference on High Voltage Engineering and Application (ICHVE), Chongqing, China, 10–13 September 2018.

10. Cheng, C.; Fu, M.; Wu, K.; Ma, Y.; Hao, Y.; Chen, C. Aging Effect on Interface Charges between Oil and Oil Immersed Paper. *IEEE Trans. Dielectr. Electr. Insul.* **2021**, *28*, 1579–1587. [CrossRef]
11. Martins, M.A.G.; Gomes, A.R. Comparative study of the thermal degradation of synthetic and natural esters and mineral oil: Effect of oil type in the thermal degradation of insulating kraft paper. *Electr. Insul. Mag. IEEE* **2012**, *28*, 22–28. [CrossRef]
12. Song, H.; Meng, H.; Yuanxin, Y.; Weiguang, Y.; Yupeng, Y.; Yuzhen, L. Influence of Electric Field Distribution on Breakdown Characteristics of Oil-paper Composite Insulation Under DC Voltage. *High Volt. Eng.* **2023**, *49*, 4938–4947.
13. Zhang, Y.; Wang, F.; Li, S.; Zhang, Y.; Li, J.; Huang, Z. Evaluation of Basic Properties and Thermal Oxidation Aging Performance for Synthetic Ester Insulating Oils. In Proceedings of the 2024 IEEE 7th International Electrical and Energy Conference (CIEEC), Harbin, China, 10–12 May 2024.
14. Wu, Y.; Lin, Y.; Wu, P.; Xu, J.; Xie, T.; Gao, C.; Hao, J. Pressure Influence Analysis of Dissolved Gas in Insulation Oil Based on Molecular Simulation and Experimental Comparsion. In Proceedings of the 2021 6th Asia Conference on Power and Electrical Engineering (ACPEE), Chongqing, China, 8–11 April 2021; pp. 756–760.
15. Perrier, C.; Marugan, M.; Beroual, A. DGA comparison between ester and mineral oils. *IEEE Trans. Dielectr. Electr. Insul.* **2012**, *19*, 1609–1614. [CrossRef]
16. Rumpelt, P.; Fritsche, R.; Bakija, B.; Jenau, F. Long-term investigations of partial discharge and gassing behavior of ester-based insulating oils for a heated oil gap. In Proceedings of the International Universities Power Engineering Conference, Heraklion, Greece, 28–31 August 2017.
17. Lashbrook, M.; Al-Amin, H.; Martin, R. Natural Ester and Synthetic Ester Fluids, Applications and Maintenance. In Proceedings of the 2017 10th Jordanian International Electrical and Electronics Engineering Conference (JIEEEC), Amman, Jordan, 16–17 May 2017.
18. Suksagoolpanya, S.; Jongvilaikasem, K.; Jariyanurat, K.; Banthoengjai, T.; Jeenmuang, S.; Pattanadech, N. Dissolved Gas Analysis of Palm Oil Compared with Mineral Oil from Different Types of Breakdown Voltage. In Proceedings of the International Conference on Condition Monitoring and Diagnosis, Bangkok, Thailand, 26–28 October 2020.
19. Suhaimi, N.S.; Ishak, M.T.; Din, M.F.M.; Ariffin, M.M.; Amin, N.A.M.; Hamid, M.H.A. Dissolved Gases Analysis of Rice Bran Oil Under Thermal Fault for Transformer Application. In Proceedings of the 2022 IEEE International Conference on Power and Energy (PECon), Langkawi, Kedah, Malaysia, 5–6 December 2022; pp. 1–6.
20. Hamid, M.H.A.; Ishak, M.T.; Ariffin, M.M.; Katim, N.I.A.; Amin, N.A.M.; Azis, N. Dissolved gas analysis (DGA) of vegetable oils under electrical stress. In Proceedings of the International Conference on High Voltage Engineering and Power Systems, Denpasar, Indonesia, 2–5 October 2017.
21. Williamson, C.; Timoshkin, I.V.; MacGregor, S.J.; Wilson, M.P.; Given, M.J.; Sinclair, M.; Jones, A. Impulsive Breakdown of Mineral Oil and Natural and Synthetic Ester Liquids When Containing Varying Levels of Moisture. *IEEE Trans. Plasma Sci.* **2021**, *49*, 466–475. [CrossRef]
22. Przybylek, P.; Gielniak, J. Analysis of Gas Generated in Mineral Oil, Synthetic Ester, and Natural Ester as a Consequence of Thermal Faults. *IEEE Access* **2019**, *7*, 65040–65051. [CrossRef]
23. Przybylek, P. Drying transformer cellulose insulation by means of synthetic ester. *IEEE Trans. Dielectr. Electr. Insul.* **2017**, *24*, 2643–2648. [CrossRef]
24. Gao, B. Molecular dynamics study on thermal decomposition characteristics of synthetic ester oil. *Chem. Phys. Lett.* **2023**, *813*, 140302. [CrossRef]
25. Tao, J.; Zhan, H.; Luo, C.; Hu, S.; Duan, X.; Liao, M. Diffusion Properties of Gas Molecules in Oil–Paper Insulation System Based on Molecular Dynamics Simulation. *Energies* **2024**, *17*, 3811. [CrossRef]
26. Ye, W.; Hao, J.; Chen, Y.; Zhu, M.; Pan, Z.; Hou, F. Difference Analysis of Gas Molecules Diffusion Behavior in Natural Ester and Mineral Oil Based on Molecular Dynamic Simulation. *Molecules* **2019**, *24*, 4463. [CrossRef] [PubMed]
27. Liu, X.H.; Men, R.J.; Jianng, W.; Li, L.; Wang, W.; Lei, Z. Molecular Dynamics Simulation of the Effects of Nano-SiO_2 Modified by Different Silane Coupling Agents on the Thermal, Mechanical and Electrical Properties of Polypropylene Nanocomposites. *High Volt. Eng.* **2025**. [CrossRef]

Disclaimer/Publisher's Note: The statements, opinions and data contained in all publications are solely those of the individual author(s) and contributor(s) and not of MDPI and/or the editor(s). MDPI and/or the editor(s) disclaim responsibility for any injury to people or property resulting from any ideas, methods, instructions or products referred to in the content.